

# Hybrid hotspot detection using regression model and lithography simulation

Taiki Kimura<sup>1a</sup>, Tetsuaki Matsunawa<sup>a</sup>, Shigeki Nojima<sup>a</sup> and David Z. Pan<sup>b</sup>

<sup>a</sup>Toshiba Corp. Semiconductor & Storage Products Company, Sakae-ku, Yokohama 247-8585, Japan

<sup>b</sup>ECE Department, Univ. of Texas at Austin, Austin, TX, 78712, USA

## ABSTRACT

As minimum feature sizes shrink, unexpected hotspots appear on wafers. Therefore, it is critical to detect and fix these hotspots at design stage to reduce development time and manufacturing cost. Currently, the most accurate approach to detect such hotspots is lithography simulation. However, it is known to be time-consuming. This paper proposes a new hotspot detection method with both a regression model and lithography simulation. Experimental results show that the proposed detection method is able to reduce computational time without accuracy loss compared to the conventional lithography simulation based hotspot detection method.

**Keywords:** hotspot, regression, optical intensity, lithography simulation, SVM, SVR

## 1. INTRODUCTION

As minimum feature sizes shrink, resolution enhancement techniques (RETs) such as high coherent illumination and complex sub-resolution assist features (SRAFs) are required to print features using 193nm immersion lithography. However, a side effect of these techniques is that optical contrast may decrease on some patterns.<sup>1</sup> Lower contrast patterns are likely to result in hotspots after etching process due to process variations. The left picture in Fig. 1 is a SEM image after lithography and the right one is a SEM image after etching. A hotspot is observed in the after-etching SEM image and such hotspot sacrifices yield at mass production stage. Therefore, it is important to detect and fix these hotspots at design stage to reduce development time and manufacturing cost. Currently, as the most accurate approach, lithography simulation is widely used to detect the hotspots. However, it is known to be time-consuming. Although several fast hotspot detection methods such as machine learning and pattern matching have been proposed,<sup>4-16</sup> those proposed methods have an unacceptable problem: their prediction accuracy is less than that of lithography simulation based methods in principle. Although computation time is important, prediction accuracy cannot be sacrificed because such hotspots cause yield loss at mass production stage. In this paper, we propose a novel hotspot detection methodology which is a hybrid of regression model and lithography simulation. It is able to produce results as accurate as lithography simulation based methods with much less computational cost.

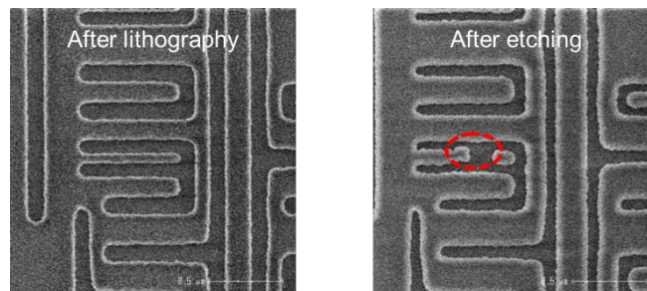


Fig. 1 Unexpected hotspot.

<sup>1</sup> Taiki Kimura: taiki2.kimura@toshiba.co.jp

## 2. BACKGROUND

### 2.1 Cause of hotspots

It has been experimentally confirmed that lower contrast points are likely to result in hotspots after etching process due to process variations.<sup>1-3</sup> A photoresist is a light-sensitive material which is dissolved by light. At resist patterns, optical intensity must be low enough to keep enough resist thickness. On the other hand, at space patterns, the intensity must be high enough to dissolve resist completely. The upper dashed line in Fig. 2 corresponds to the threshold for under exposure dose, which is defined by process variations and the lower dashed line corresponds to the threshold for over exposure dose. The high contrast image in the left of Fig.2 shows the peak of the optical intensity is higher than the threshold for under. This means pattern can print the space properly. However, peak intensity of the low contrast image in the right of Fig.2 is less than the threshold and this leads to photoresist bridging and a fail after etching process. Similarly pattern cannot keep enough resist thickness when the bottom intensity is higher than the threshold for over as shown in the right of Fig 2.

Therefore, to detect such hotspots, calculating optical intensity using lithography simulation and judging if the value is lower or higher than the pre-determined threshold are required.

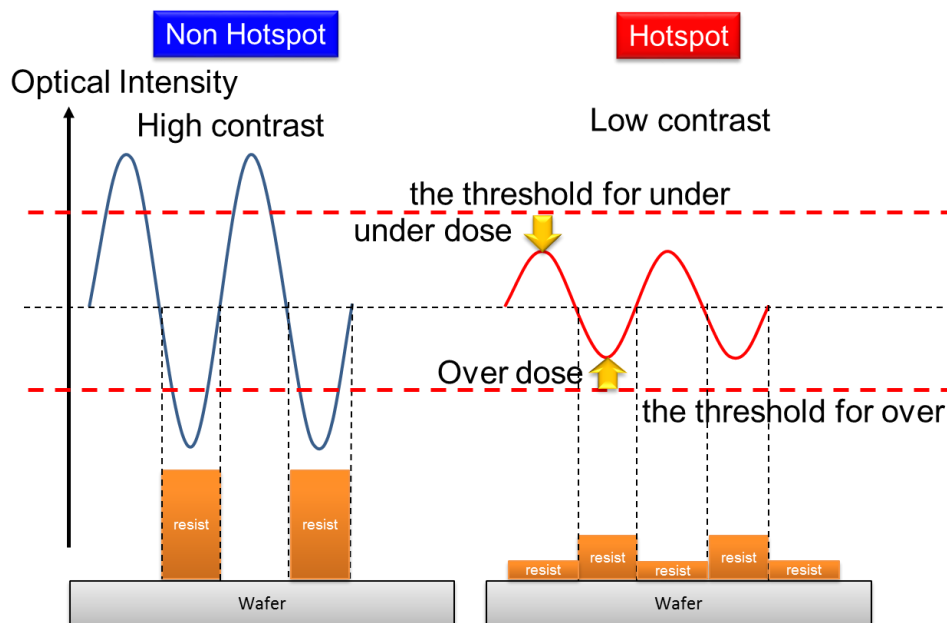


Fig.2 Cause of hotspots

### 2.2 Conventional hotspot detection

Fig.3 shows conventional aerial image calculation flow. It is necessary to calculate an aerial image for a whole layout to detect where the optical intensity is lower or higher than the threshold. However, aerial image calculation takes longer time when the size of a lithography simulation unit defined by optical diameter is large and it is impossible to calculate the aerial image of the whole layout at one time. Firstly a whole layout is divided into small clipped patterns. To accurately calculate optical intensity at the center point of the clipped pattern, the size of each clipped pattern is to be larger than the optical diameter in optical principle. Secondly, optical intensity of the center of each clipped pattern is calculated using lithography simulation which is a very time consuming process. Then, the aerial image of the whole layout is synthesized, tiling the individually calculated optical intensity. Finally, the calculated intensity is tiled to their original positions

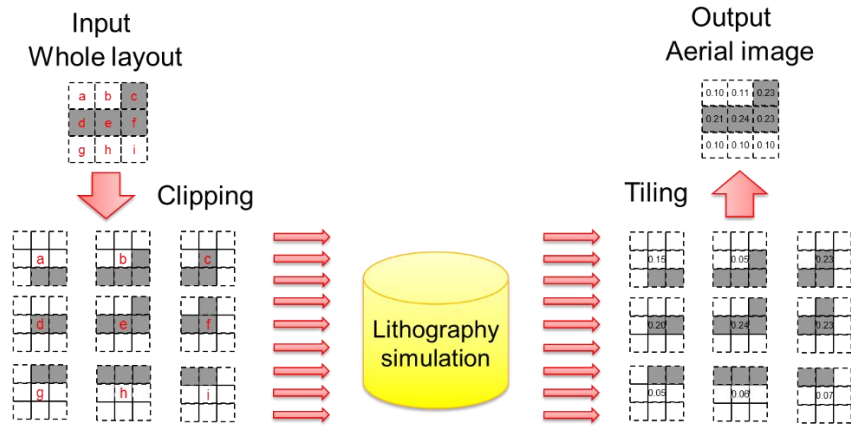


Fig.3 Conventional aerial image calculation flow

The aerial image is used to determine the location of hotspots, as shown in Fig.4. Firstly, the orange point is extracted as contour from the aerial image at the specified threshold. In this example, the threshold for under is 0.21 and the threshold for over is 0.14. The contour is compared with the original layout to extract differences between the contour and original layout. The extracted point which has lower intensity than the specified threshold is detected as an under hotspot. Similarly, the extracted point which has higher intensity than the specified threshold is detected as an over hotspot. The exact location of the hotspots can be identified using this method. But it is time-consuming because lithography simulation is slow.

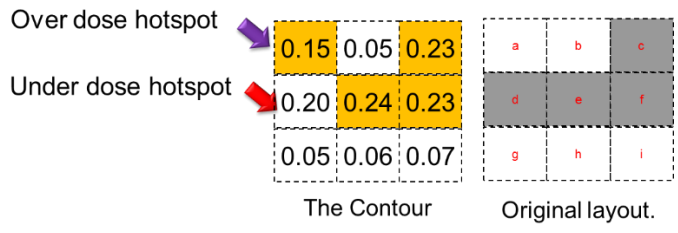


Fig.4 Conventional method flow

### 3. HYBRID HOTSPOT DETECTION METHOD

#### 3.1 Concept of the proposed method

In Fig.5, the upper figure shows a conventional method, and the lower one shows our method. The key point of speed-up is how to reduce the lithography simulation times. To realize this, our method uses a hybrid between regression model and lithography simulation. As shown in Fig. 5, the hybrid method first uses a regression model to predict optical intensity, and then a part of the prediction results are recalculated with the true results from lithography simulation. A reduction of calculation time is realized by replacing the lithography simulation, which is a time-consuming procedure, with the regression model, which is a fast prediction technique. Obviously, the same aerial images cannot be achieved by the hybrid method since it includes a regression function. However, as discussed later, our method can get contour images that are equivalent to the contour calculated by lithography simulation.

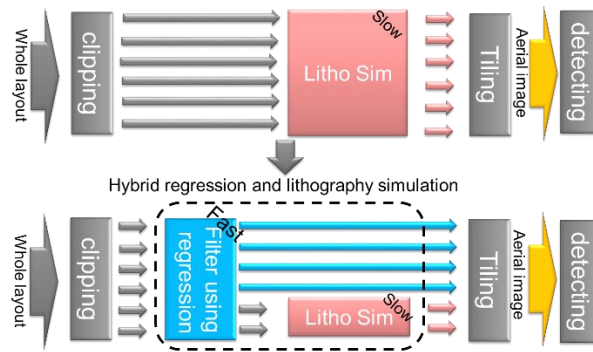


Fig.5 Concept of proposed method.

Fig. 6 shows a relation between predicted intensity using regression and true intensity from lithography simulation. One dot corresponds to one clipped pattern. The predicted value has an error range due to the accuracy of regression model. Suppose the regression model has a strong correlation with lithography simulation, we can ignore the effect of the error range of the predicted value when the predicted value is far from the specified threshold. This means that there is no possibility of misjudgment, whether the predicted value is lower or higher than the specified threshold. In contrast, there is a possibility of misjudgment if it is close to the threshold. It indicates that a part of the time-consuming lithography simulations are replaceable with the regression model which is high-speed but not precise. The regression model functions as a filter. The filter determines whether the threshold exists within the error range of the predicted value.

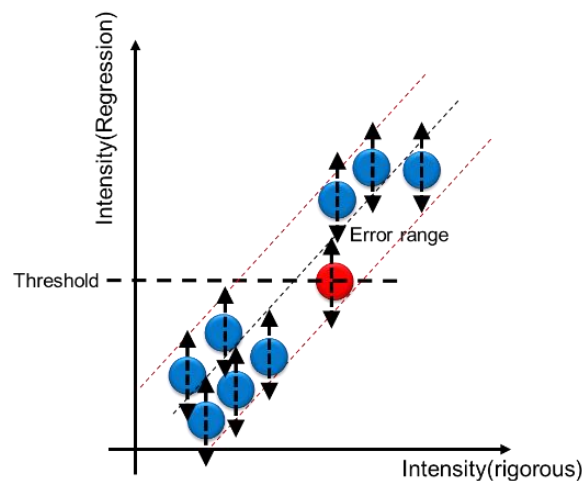


Fig. 6 Relation between the regression results and rigorous results.

### 3.2 Regression model

Fig.7 shows our regression flow. We first train a regression model using training patterns and lithography simulation, and then optical intensity of a test pattern is predicted using the model. The input of the model is extracted layout features, and the output is predicted intensity value at the center of a test pattern. In this paper, we adopt support vector regression (SVR) with Gaussian kernel as the regression model. In the following, layout feature extraction method and the basic idea of kernel selection are briefly described in the following chapters.

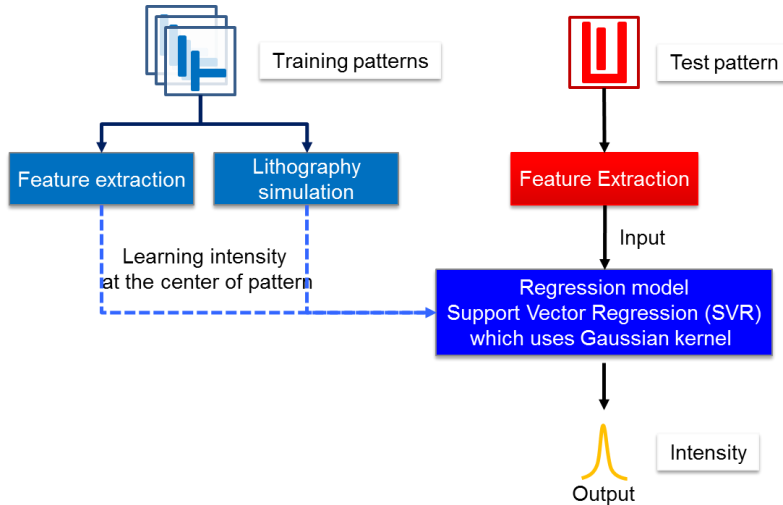


Fig.7 Regression flow.

### 3.2.1 Feature extraction

It is difficult to handle the input layout directly because of its high-dimensional space. CCAS (concentric circle area sampling) is used as the feature extraction method to degrade the dimension. The influence of the diffracted light decreases with the distance from the center point. Fig.8 explains the basic concept of CCAS using "F" shaped test pattern. Red points are sampling points. Parameters of the feature consist of the total size of the encoding area  $l$  and the sampling density controlling parameter  $r_{in}$ . The radius of the concentric square is  $0, 4, 8, r_{in}, r_{in} + 8, r_{in} + 16, \dots, l/2$  pixels, respectively. The subsampled pixel values in CCAS correspond to the influence of the diffracted light decreases concentrically. The layout feature is a density of pattern which is subsampled concentrically. The sampling density decreases with the distance from the center point. Therefore, CCAS is a reasonable feature extraction method for optical intensity regression model. A feature vector  $\mathbf{x}$  contains subsampled pixel values on concentric circle of layout patterns.

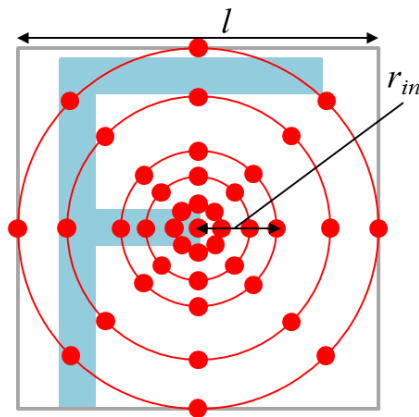


Fig.8 Concentric circle area sampling (CCAS)

### 3.2.2 Kernel selection for SVR

The regression equation using SVM is described as the Eq. (1), where  $y^i$  is the predicted result,  $\mathbf{x}^i$  is the feature vector of the prediction target,  $\mathbf{x}^j$  are the support vectors, and  $k$  is a kernel of a transformation. Although several kernel functions, such as Linear, Polynomial and Gaussian kernel, can be used, this paper takes Gaussian kernel because Gaussian kernel based SVR model can be regarded as a SOCS approximation. Specifically, the SVR model is given by

$$y^i = \sum_j \alpha_j \phi(\mathbf{x}^i) \cdot \phi(\mathbf{x}^j) = \sum_j \alpha_j k(\mathbf{x}^i, \mathbf{x}^j) \quad (1)$$

This equation can be written in the form

$$y^i = \sum_j \alpha_j k(x^i, x^j) = \sum_j \alpha_j \exp(-\beta \|x^i - x^j\|^2) = \sum_{k=1}^1 \lambda_k f(x^i) \otimes g(x^i) \quad (2)$$

where  $\lambda_1 = 1$ . The following equation shows the Sum Of Coherent Systems(SOCS) approximation of Hopkin's imaging.

$$I(x) = \sum_k \lambda_k |\phi_k(x) \otimes M(x)|^2 \quad (3)$$

where  $\phi_k(x)$  is SOCS kernel and  $M(x)$  is mask pattern. Both equations, (2) and (3), have a similar formation. In the Eq. (3), one mask pattern is convoluted with some of the kernels which are based on the source shape of illumination. On the other hand in Eq. (2), some of the support vectors which are selected by SVM are convoluted with one kernel function which is Gaussian. Where the support vector is the feature of the mask pattern. It is interpreted that SVM conjectures the source shape of illumination and select the support vector. Therefore the SVR which uses Gaussian kernel is a rough approximated expression of optical intensity.

## 4. EXPERIMENTS

In this section, we first train a regression model with Gaussian kernel based SVR. The aerial images of input layouts are then synthesized using the hybrid method based on the combination of regression model and conventional lithography simulation. Besides, predicted intensity values are compared with true intensities from lithography simulation to confirm the performance of regression model. The proposed methods are implemented in C and C++ on a Linux machine. The simulation conditions are as follows: wavelength  $\lambda = 193\text{nm}$ ,  $\text{NA} = 1.35$ , source shape of illumination as quad poles, and optical diameter as  $2.8\mu\text{m}$ . For regression model training, 10,000 patterns are extracted in a random manner from ICCAD 2012 benchmarks. As shown in Fig.9, we clipped arbitrarily three areas which are  $1.2\mu\text{m}^2$  from ICCAD 2012 benchmarks as test layouts, and then each test layout is divided into  $120 \times 120$  patterns. We extracted pattern features from the training and test patterns with CCAS, where  $l = 1.2\mu\text{m}$ ,  $r_{in} = 150\text{nm}$ , and the dimensions of feature vector is 257.

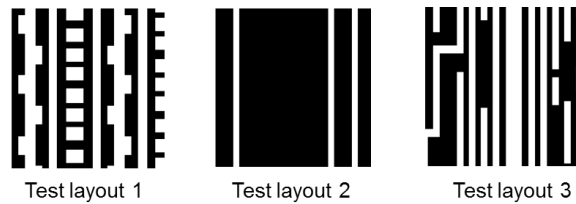


Fig. 9 Test layout.

### 4.1 Regression results

As mentioned in Section 3, the proposed regression model predicts optical intensity of the center point on an input pattern using extracted layout features. To evaluate the generalization capability of regression, predicted intensities are compared with true intensities obtained by lithography simulation. Fig.10 represents a relation between regression and lithography simulation. One dot corresponds to one pattern. In the figure, (a) and (b) represent the training result (interpolation) and testing result (extrapolation), respectively. Both results indicate a strong correlation between regression and lithography simulation.

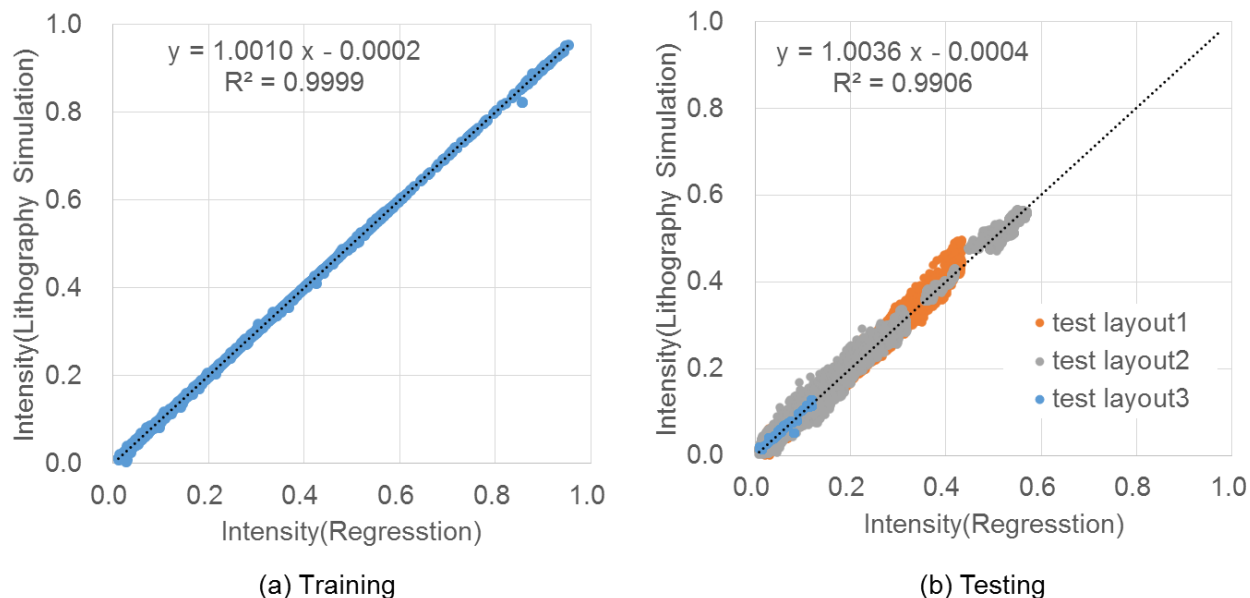


Fig. 10 SVR results. (a) Training. (b) Testing.

#### 4.2 Extracting contour from synthesized aerial image

The contour image is extracted from the aerial image at the specified threshold (See Section 2.2). Fig. 11(a) and (b) represent synthesized aerial image of test layout 1 calculated only by lithography simulation and its contour image, respectively. Also, Fig. 11(c) and (d) indicate synthesized aerial image of test layout 1 obtained by proposed hybrid method and its contour image, respectively. In this experiment, the threshold is 0.21, and a regression to lithography simulation ratio is 83% to 17%. From the figure, we can see that although the aerial images are different, the extracted contours are exactly the same. Similarly, Fig.12 shows results of lithography simulation and proposed method for test layout 2 and test layout 3. In both results, it can be seen that the same contours as the results of lithography simulation are achieved as well from our hybrid method although the aerial images are different. This indicates that an accurate contour image can be obtained in short runtime by using the hybrid method.

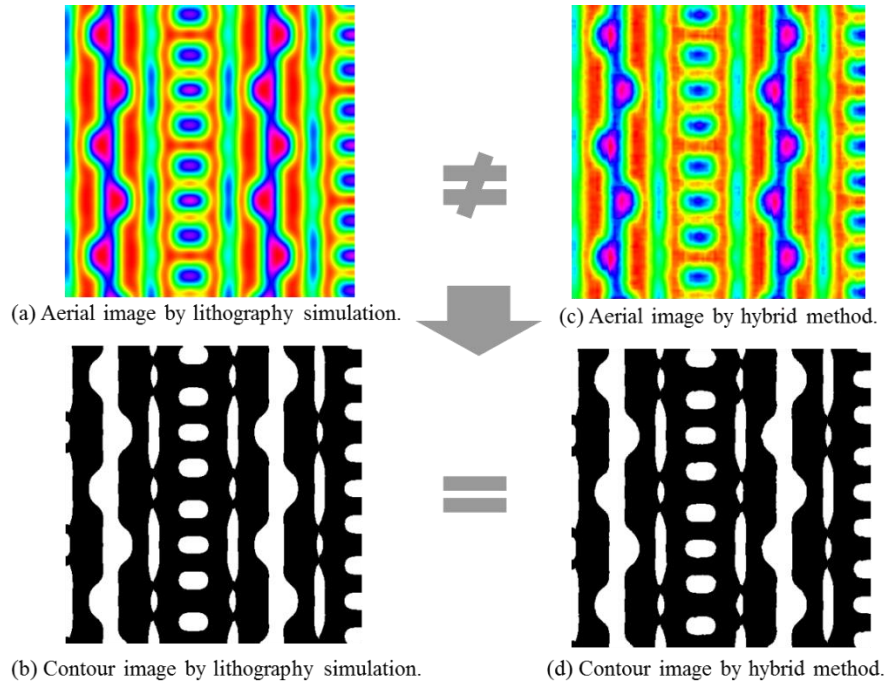


Fig.11 Aerial and contour images of test layout 1. (a) Aerial image by lithography simulation. (b) Contour image by lithography simulation. (c) Aerial image by hybrid method. (d) Contour image by hybrid method.

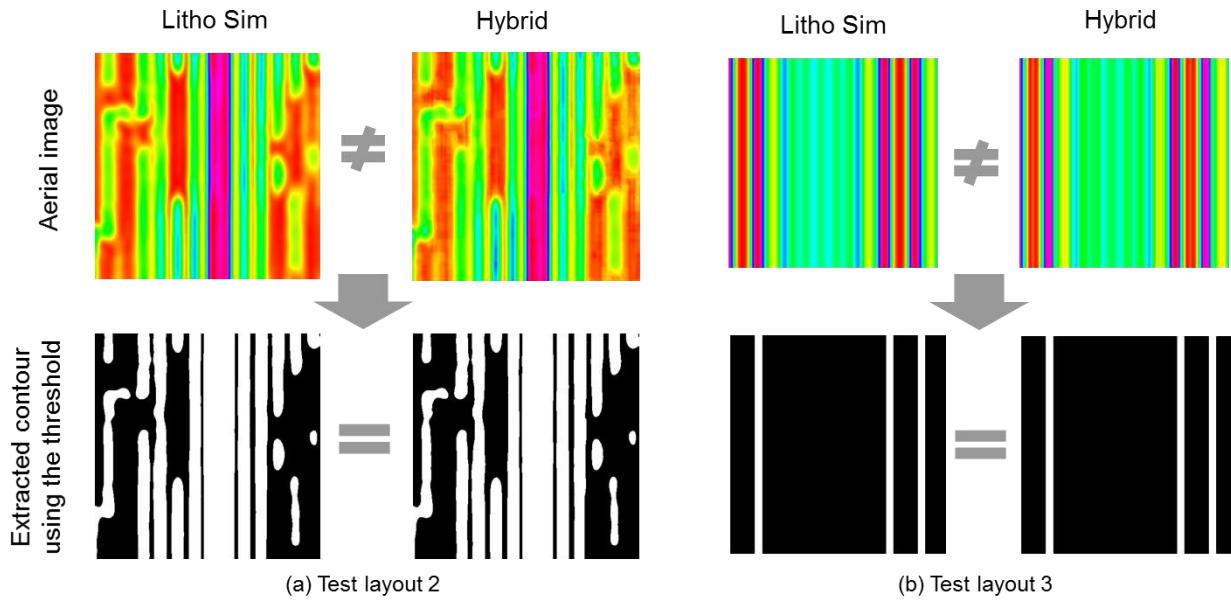


Fig.12 Aerial and contour images of test layout 2 and 3. (a) Test layout 2. (b) Test layout 3

### 4.3 Hotspot detection

Based on the contours obtained in the previous experiment and the method discussed in Section 2.2, we detect hotspots from test layout 1. Fig. 13 (a) indicates the original layout and (b) shows the contour image calculated by the hybrid method. The red circles in the figure represent detected hotspots because the extracted points are disconnected compared to the



original layout. It should also be noted that this detection result is exactly the same as the result of conventional hotspot detection method since the same contours as lithography simulation can be achieved by the hybrid method.

Fig. 14 represents the runtime of conventional method and our method. As shown in the figure, our new method produces results as accurate as full lithography simulation with 70% less computational time

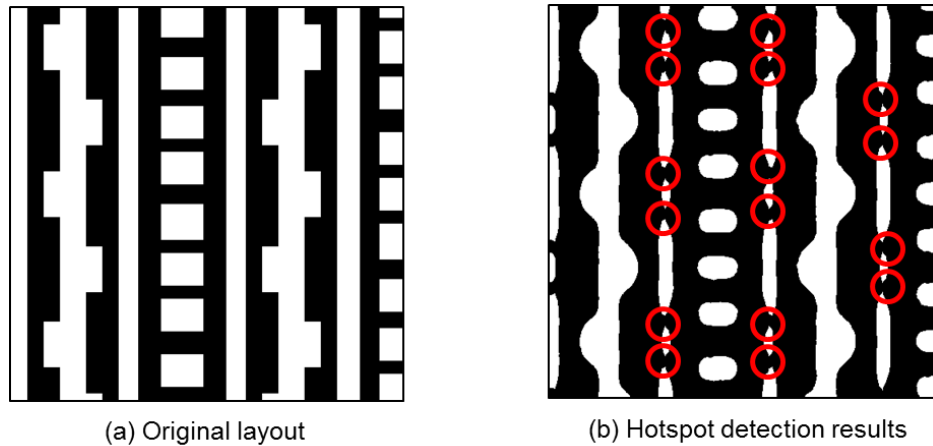


Fig.13 Hotspot detection results. (a) Original layout. (b) Hotspot detection results.

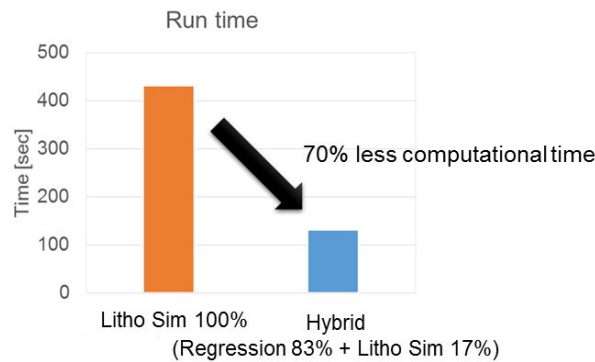


Fig.14 Runtime comparison.

## 5. CONCLUSION

We developed a new hotspot detection method using a hybrid of regression model and lithography simulation. The Gaussian kernel based support vector regression (SVR) can provide a good approximation to the true optical intensity calculation. Thus, most time-consuming lithography simulation are replaceable with the SVR which is a faster prediction model. We can get exactly the same detection results compared to the conventional lithography simulation based hotspot detection method while reducing the calculation time. Experimental results demonstrate that our new method is able to produce results as accurate as full lithography simulation with 70% less computational time.

## REFERENCES

- [1] Kimura, T., et al., "Hotspots prediction after etching process based on defect rate" Proc. of SPIE, 9426 (2015)
- [2] Dongho K., et al. "Full Chip Model Based OPC Verification by using Rigorous Resist 3D Model" Proc. of SPIE, 9052 (2014)
- [3] Qing Y., et al. "3D Resist Profile Full Chip Verification and Hot Spot Disposition" Proc. of SPIE, 8683 (2013)

- [4] Matsunawa, T., et al., "A new lithography hotspot detection framework based on AdaBoost classifier and simplified feature extraction" Proc. of SPIE, 9427 (2015)
- [5] Nagase, N., et al., "Study of hot spot detection using neural network judgment," in Proc. of SPIE, 6607 (2007)
- [6] Wu, J.-Y., et al., "Detecting context sensitive hot spots in standard cell libraries," in Proc. of SPIE, 7275 (2009).
- [7] Drmanac, D.G., et al., "Predicting variability in nanoscale lithography processes," in IEEE/ACM Design Automation Conference (DAC), 545-550 (2009)
- [8] Ding, D., et al., "Machine learning based lithographic hotspot detection with critical-feature extraction and classification," in IEEE International Conference on IC Design and Technology (ICICDT), 219-222 (2009)
- [9] Wu, J.-Y., et al., "Rapid layout pattern classification," in IEEE/ACM Asia and South Pacific Design Automation Conference (ASPDAC), 781-786 (2011).
- [10] Ding, D., et al., "High performance lithographic hotspot detection using hierarchically refined machine learning," in IEEE/ACM Asia and South Pacific Design Automation Conference (ASPDAC), 775-780 (2011).
- [11] Wu, J.-Y., et al., "Efficient approach to early detection of lithographic hotspots using machine learning systems and pattern matching," in Proc. of SPIE, 7974 (2011).
- [12] Mostafa, S., et al., "Multi-selection method for physical design verification applications," in Proc. of SPIE, 7974 (2011).
- [13] Ding, D., et al., "EPIC: Efficient prediction of ic manufacturing hotspots with a unified meta-classification formulation," in IEEE/ACM Asia and South Pacific Design Automation Conference (ASPDAC), 263-270 (2012).
- [14] Yu, Y.-T., et al., "Machine-learning-based hotspot detection using topological classification and critical feature extraction," in IEEE/ACM Design Automation Conference (DAC), 671-676 (2013).
- [15] Lin, S.-Y., et al., "A novel fuzzy matching model for lithography hotspot detection," in IEEE/ACM Design Automation Conference (DAC), 681-686 (2013).
- [16] Gao, J.-R., et al., "Accurate lithography hotspot detection based on pca-svm classifier with hierarchical data clustering," in Proc. of SPIE, 90530E-90530E (2014).